I&EC research
Industrial & Engineering Chemistry Research

pubs.acs.org/IECR
Article

Tailings as a Source for Generating Valuable Magnesium and Calcium Carbonates by Leaching and Carbonization

Volker Bächle,* Chinmay Laxminarayan Hegde, Andreas Voigt, Kai Sundmacher, and Marco Gleiß*

Cite This: *Ind. Eng. Chem. Res.* 2025, 64, 12064−12073

ABSTRACT: Mining produces a lot of disposable mineral waste after the ore has been removed. This waste with added CO_2 can be used as a feedstock for carbonate production. The advantage of this production process is the recycling of a waste product with additional carbon capture. However, the processing challenge is a feed with a fluctuating composition of the mining waste, which makes classical engineering and control with fixed process parameters difficult. For characterization, model particles and tailings are studied for their behavior with fluctuating acid and mass concentrations as a function of the leaching time. The results confirm the possibility of leaching calcium (max 7 g L^{-1}) and magnesium (max 0.7 g L^{-1}) using hydrochloric acid with concentrations lower than the stoichiometry. The amount varies depending on the particle, concentration, and pH. Mathematically, the leaching over time can be described by an exponential expression, which is applied to both investigated cases for the leaching of calcium and magnesium ions. Finally, a pH shift process is used to precipitate solid $CaCO_3$ from the ion-enriched solution obtained, thus demonstrating in one example the successful production of $CaCO_3$ and carbon capture from mine waste.

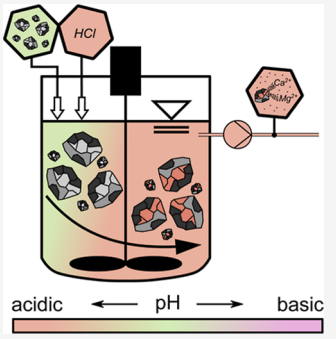

INTRODUCTION

Carbonates are important raw materials in many areas of the industry. Today, precipitated calcium carbonate (PCC) in particular can replace the natural mineral $CaCO_3$. PCC is used in coating pigments and fillers in rubber, plastics, paints (15 Mt/a), and paper (10 Mt/a).[1−4] $CaCO_3$ is conventionally produced from limestone, which consists mainly of $CaCO_3$ in addition to magnesium carbonate $MgCO_3$ and other compounds.[5] Naturally occurring limestone reserves are available all over the world and are mined in large quantities, which has an impact on the environment. Alternatively, $CaCO_3$ can be produced synthetically as a PCC. In the first step, quicklime (CaO) is deglazed by reacting with water (H_2O) to form calcium hydroxide ($Ca(OH)_2$). CO_2 is passed through the $Ca(OH)_2$ solution to produce PCC and H_2O. This process is known as carbonation. The reverse process, calcination, is used to make quicklime. $CaCO_3$ decomposes to CO_2 and CaO in a thermolysis process that requires a large amount of thermal energy.[4,6−9]

In terms of climate protection, it is particularly important that raw materials such as $CaCO_3$ are produced in an environmentally friendly and resource-saving manner. One possibility for carbon capture to limit anthropogenic warming is to inject CO_2 into sedimentary basins which requires an impermeable cap rock to prevent CO_2 from migrating to the surface.[10] Inside the basin, carbon mineralization takes place, but with this technology, the generated product cannot be used and is only permanently stored. As a result, lime is still mined. Therefore, technologies that bind greenhouse gases in addition to the production of raw materials are important components in fighting climate change. In addition to the leaching of lime, recycling of waste streams is a variant of energy-saving carbonate production. In industry, there are many waste streams that are rich in calcium, for example, there is cement waste (1 Gt/a) coal fly ash (750 Mt/a), steel mill slag (400 Mt/a), and mine tailings (77 Mt/a).[11−14] The food sector also produces waste streams containing calcium, such as eggshells, which can be used for calcium leaching.[15] While there is research on the recovery of calcium from cement waste,[16] coal fly ash,[17] and steel mill slag,[18] research on tailings as a raw material is more limited to heavy metals.[19,20] As the most common alkaline earth metals in nature, calcium and magnesium are also present in tailings, and they are useful raw material for carbonates.[21] One potential approach for carbonation is the pH swing method, which emulates the natural chemical weathering process. Gerdemann et al. describe this pathway for carbon capture as "ex situ" aqueous mineral carbonation, which refers to carbonation above ground.[22] Not all mining wastes have a high carbonation potential. This is part of the work of Hitch et al., who are characterizing and modeling the carbon sequestration behavior of various mining wastes.[23−26] To utilize the carbonates produced, indirect carbonation must take place, which involves an additional step of extracting the reactive solid compounds.[11]

Received: February 24, 2025
Revised: May 14, 2025
Accepted: May 16, 2025
Published: June 9, 2025

https://doi.org/10.1021/acs.iecr.5c00797
Ind. Eng. Chem. Res. 2025, 64, 12064−12073

To improve the reaction kinetics, pretreatment can be performed by thermal, mechanical by milling,[27] or chemical means.[28] For magnesium extraction, sulfuric acid is a commonly used extraction agent that can extract more than 70% from serpentine. However, chemical activation tends to form silica gel, which can trap the necessary cations required for carbonation.[28] Current research focuses on wollastonite, serpentine, and olivine.[29] Subsequent to leaching, the calcium (Ca^{2+}) and magnesium (Mg^{2+}) ions present in the tailings are carbonized with CO_2 to form $CaCO_3$ and $MgCO_3$.[8,30,31] This process represents an energy-saving, sustainable, and environmentally friendly alternative to previous production methods as tons of mine waste produced each year are refined and CO_2 is captured from the atmosphere. Mineral carbonation can thus contribute to the reduction of CO_2 in the atmosphere, which is one of the main causes of global warming, and can provide sustainable and geostable CO_2 storage in carbonates.[8,30,32,33]

The key factors preventing the successful use of aqueous mineral carbonation on a large scale are high operating costs, energy intensity, slow reaction, and low carbon dioxide fixation efficiency.[29] In order to achieve high efficiency for energy input, cost of operation, and wide applicability, it is proposed to develop an autonomous process capable of adapting to the specific conditions of each mine. The process is composed of four distinct stages: leaching, filtration, precipitation, and separation. The leaching stage involves the dissolution of alkaline ions from minerals, while the filtration stage with a vacuum belt filter is responsible for separating solid residues. Vacuum belt filters have better cake washing properties compared to those of other filtration devices in order to retain all of the ion-enriched liquid. This filter is also scalable to large processes in the mining industry.[34] The precipitation stage is responsible for the selective production of carbonates in a closed tank, and finally, the centrifugation stage is responsible for separating the carbonates from the precipitating solution. These steps are necessary to obtain high purity carbonates. In situ carbonation with direct carbonation is simpler in the process, but the carbonates are contaminated with the original mine waste and therefore not useable for the industry. Carbonation without pH swing is also possible but less effective as alkaline conditions favor the carbonation process.[29] The advantage of this method is that each step can be optimized separately.[35] This study focuses on the initial step, namely, the leaching of Ca^{2+} and Mg^{2+} ions from a range of minerals with the main focus on Ca^{2+}. The quality of the leaching is determined by means of ion chromatography, with the analysis conducted at varying times of acid addition. The following acids are employed: hydrochloric acid (HCl), sulfuric acid (H_2SO_4), and citric acid ($C_6H_8O_7$). In addition to real tailings from an iron and copper mine, the individual particles of anhydrite and talc are examined for comparison between single and multiple particle systems. The objective is to characterize the process of acid leaching with regard to autonomous control by identifying the optimal acid type, acid concentration, and leaching time for continuous, autonomous control to produce selective carbonates of $CaCO_3$ and $MgCO_3$ with high purity using the pH swing carbonation method.

MATERIALS AND METHODS

Sample Preparation and Characterization. The calcium-containing compound used is the product anhydrite Trefil 1313-100 with $x_{50,3}$ = 6.8 μm from Quarzwerke GmbH (Frechen, Germany). Trefil consists of 98.4% calcium sulfate by mass and is therefore a mineral that is suitable for dissolving Ca^{2+} ions. Talc EX-GT-10 with $x_{50,3}$ = 5.7 μm (mean particle diameter) from Quarzwerke GmbH is used for the magnesium content in the particle mixture. This talc has a magnesium oxide content of 31%, with the remainder being bound by silicates. The particle size is determined by laser diffraction spectroscopy on an LBS Helos Quixel from Sympatec GmbH (Clausthal-Zellerfeld, Germany). The chemical compositions of the particles are listed in Table S1 (Supporting Information). In addition, the chemical reactions with hydrochloric acid to form soluble ions are listed as examples.

$$\text{Anhydrite: } CaSO_{4(s)} + 2HCl_{(aq)} \rightleftarrows CaCl_{2(aq)} + SO_4^{2-}{}_{(aq)} + 2H_{(aq)}^{+} \quad (1)$$

$$\text{Talcum: } Mg_3Si_4O_{10}(OH)_{2(s)} + 6HCl_{(aq)} \rightleftarrows 3MgCl_{2(aq)} + 4H_2O_{(l)} + 4SiO_{2(s)} \quad (2)$$

In addition to the particles and deionized water, acid is required for leaching. Hydrochloric acid 30% technical (HCl) from VWR International GmbH (Darmstadt, Germany), sulfuric acid 96% technical (H_2SO_4) from Carl Roth GmbH + Co. KG (Karlsruhe, Germany), and citric acid ($C_6H_8O_7$) were obtained from Carl Roth GmbH + Co. KG (Karlsruhe, Germany) are used. The three acids are added in different stoichiometric ratios (St). The ratio is defined by the following equation with the amount of used acid in the experiments (3)

$$St = \frac{m_{acid,used}}{m_{acid,required}} \quad (3)$$

$m_{acid,required}$ is the theoretical amount of acid required to completely dissolve the alkaline ions according to the chemical reactions (1) and (2). 30 % hydrochloric acid and 96% sulfuric acid are added to the anhydrite in the ratios St 1, 0.5, and 0.2. Citric acid is only added in a stoichiometric ratio of 1, as this is a weaker acid compared to hydrochloric and sulfuric acid. The stoichiometric ratios can be found in the reaction eqs 1 and 2 in Table S1.[36−38] For sulfuric acid and citric acid, complete protonation ($H_2SO_4 \Rightarrow 2H^+$ and SO_4^{2-}; $C_6H_8O_7 \Rightarrow 3H^+$ and $C_6H_5O_7^{3-}$) is assumed. H_2SO_4 does not react with anhydrite because both reactants form sulfate ions, but a change in pH can affect the solubility. This allows characterization of the pH dependence on ion saturation. Citric acid, similar to H_2SO_4, does not dissolve anhydrite but can alter the microstructure of gypsum formed in aqueous environments.[39,40]

In addition to the synthetic particle systems, two tailings from an iron mine and a copper mine in the northern United States are analyzed. The composition of the tailings is listed in Table S2 (Supporting Information) in mass fractions quantified by wavelength dispersive X-ray fluorescence (S4 Explorer, Broker, Bruker Co, Billerica, USA). Since no explicit reaction equations can be established for multicomponent mixtures, the calculation is based on the identical amount of acid for anhydrite. Thus, for anhydrite and for both tailings, 5% w/w and St 1.0 corresponds to a molar HCl concentration of 0.75 M. Accordingly, St 0.5 also corresponds to half the acid concentration. It should also be mentioned that the proportion of CaO within the copper tailing consists of gypsum, which corresponds to anhydrite.

https://doi.org/10.1021/acs.iecr.5c00797
Ind. Eng. Chem. Res. 2025, 64, 12064−12073

To compare the individual materials, the measured values of Ca and Mg are normalized to the theoretically maximum achievable value $c_{i,max}$ and displayed as C_i^*

$$C_i^* = \frac{c_{i,measured,IC}}{c_{i,max}} \quad (4)$$

where $c_{i,measured,IC}$ is the measured ion concentration of Ca or Mg by ion chromatography. $c_{i,theomax}$ is the calculated concentration of calcium and magnesium, given the composition described in Tables S1 and S2, when all the calcium and magnesium available are in solution. The calculated maximum concentrations are given in Table S3 (Supporting Information) for 5 mass percent.

Fabric 07-1500-SK 011 from SEFAR AG (Heiden, Switzerland) is used for the experiments. It is made of poly(ethylene terephthalate) (PET) and is therefore suitable for the low pH values of the leaching. The mesh is responsible for coarse filtration of the solids. The filtrate is then filtered again using a ROTILABO syringe filter with a pore size of 0.45 μm made of cellulose acetate from Carl Roth GmbH + Co KG (Karlsruhe, Germany) for ion chromatography.

To describe the leaching, a simple mass balance is set up around the minerals, calcium and magnesium. One assumption is that it is a batch process, with no ingoing or outgoing process streams. Thus, only the chemical reaction is considered. Furthermore, no volume change occurs during leaching; therefore, the mass balance can be converted into a concentration balance. The amount of material used in the batch process at the beginning is described in the constant $C_{\infty,i}$

$$\frac{dC_i(t)}{dt} = k_i(C_{\infty,i} - C_i(t)) \quad (5)$$

To solve eq 5, the integral is formed over the concentration $C_i(t)$ and the kinetic parameter over time. The solution is an exponential function with $C_{\infty,i}$ as the upper limit of the soluble ions. After fitting the function to the data, the value of $C_{\infty,i}$ can therefore not exceed the values in Table S3. Solid components cannot react because they also have diffusive character. Diffusion within the particles is not considered in this work. As a result, $C_{\infty,i}$ can be lower than the value after fitting the equation to the data. $C_{0,i}$ corresponds to the concentration at the beginning of the leaching process, and k corresponds to the reaction rate. Equation 6 can be used for both alkaline ions calcium and magnesium

$$C_i(t) = C_{\infty,i} - (C_{\infty,i} - C_{0,i})e^{-k_i t} \quad (6)$$

EXPERIMENTAL SETUP AND PROCEDURE

The leaching takes place on a laboratory scale using a glass container made of borosilicate glass with a filling volume of 100 mL of suspension; see Figure 1. First, a mixture of deionized water and the particles with a mass fraction between 5 and 15% w/w is prepared. The sample is then taken without acid, which corresponds to the leaching value at 0 h. The value of ion concentration without acid determines the solubility of the particles in water. Acid is then added with continuous stirring using a propeller stirrer.

To characterize the leaching rate with HCl, tests are performed on all particles at 0 min (no acid addition), 30 min, 1, 3, 5, 8, and 24 h. The acid concentrations for all particles are based on the stoichiometric ratio for anhydrite and are St = 0, 0.2, 0.5, and 1. For anhydrite and talc, mass concentrations of

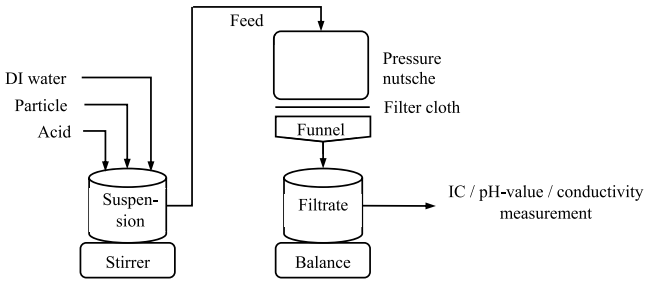

Figure 1. Schematic diagram of the experimental setup with leaching on the left side and filtration for characterization on the right side.

10% and 15% are also considered. Anhydrite is the calcium component of the copper mine. Therefore, in contrast to the other particles, additional tests are performed on anhydrite using the different acids HCl, H_2SO_4, and citric acid. The leached samples are filtered through the above-mentioned filter medium from Sefar GmbH (manufacturer name 07-1500-SK 011, Edling, Germany) with a filter area of 0.00196 m^2 using a pressurized filter cell according to VDI Guideline 2762-2, and the solution is filtered again through a syringe filter with 0.45 μm pore size.[41] Direct filtration with a membrane is not possible due to the high solids concentration of more than 5% w/w. Afterward, the current particle-free solution is analyzed on an ion chromatograph from Metrohm AG (Herisau, Switzerland) using the Metrosep C 6-150/4.0 separation column. At the same time, the conductivity of the suspension is measured using the WTW Cond 340i conductivity meter (Weilheim, Germany). The conductivity can be used to estimate the kinetics of the solubility of particles in deionized water. This is not possible using the ion chromatograph as the manual process via the syringe filter is not feasible in terms of time.

The particle-to-acid concentration ratios vary between 0 and 1.0 with St = 0 for the experiment without acid. It is not the objective to achieve a stoichiometric ratio St above 1, given that the particles are present in large quantities in tailings and the use of acid represents an additional expense. Accordingly, the acid utilized in the experiments is restricted to St = 1.

RESULTS

Influence of the Leaching Acid. Figure 2 shows the ion concentrations for the various acids and their stoichiometric ratio. The concentration of Ca^{2+} ions is shown at different times for leaching with 5% w/w anhydrite. The concentration of Ca^{2+} ions increases in the first 30 min and then hardly changes. Thereafter, the ion concentration remains constant; consequently, no further Ca^{2+} ions are dissolved, and the acid leaching is complete. The initial value at 700 mg L^{-1} is noticeable. This corresponds to the solubility of anhydrite in deionized water at 20 °C. According to Lide et al., the solubility product of $CaSO_4$ is 4.93×10^{-5} mol^2 L^{-2} at 20 °C, which corresponds with the molar mass of calcium sulfate to 956 mg L^{-1} in water and is therefore slightly higher than the measured values.[42] No increase in Ca^{2+} concentration can be observed with sulfuric acid. When calcium is dissolved from the anhydrite in water, SO_4^{2-} is released as an anion, which is also the product of the reaction with sulfuric acid. The equilibrium of this reaction is therefore already present due to the saturation of SO_4^{2-} in water, which is why sulfuric acid cannot dissolve any further ions from the crystal. In this case, the pH value also has no influence on the saturation of

https://doi.org/10.1021/acs.iecr.5c00797
Ind. Eng. Chem. Res. 2025, 64, 12064−12073

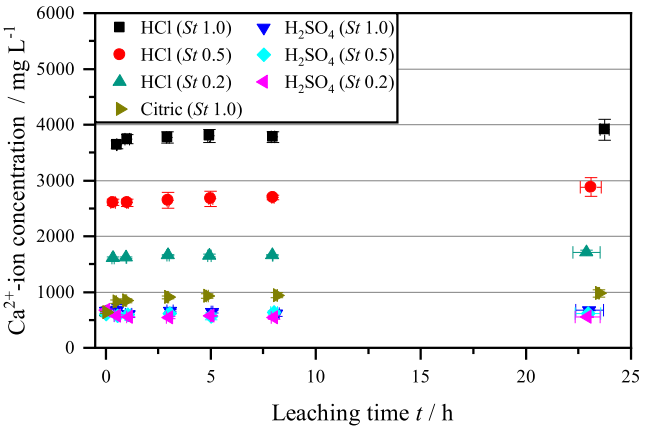

Figure 2. Concentration of Ca^{2+} ions after leaching from anhydrite suspensions with a mass fraction of 5% w/w as a function of leaching time and acid concentrations. The investigated acids are hydrochloric acid (HCl), sulfuric acid (H_2SO_4), and citric acid.

anhydrite, as there is no change in the ion concentration even with different acid concentrations in the stoichiometric ratios St between 0.2 and 1. Therefore, this acid is not treated in the further course of this investigation, which focuses primarily on Ca^{2+}. In comparison, the dissolved calcium content of hydrochloric acid continues to increase with increasing acid concentration. For example, after 24 h, the Ca ion concentration at St 1.0 is 3916 mg L^{-1}, whereas the concentration at St 0.5 is 2888 mg L^{-1} and at St 0.2 1717 mg L^{-1}. In comparison between St 0.2 and St 1.0, the ion yield with a 5-fold acid input is therefore only 2.28. Between St 0.2 and St 0.5 with a 2.5-fold acid input, there is an increase of 1.68. The yield to the acid input ratio therefore increases with decreasing acid concentration. Noticeable is the solubility product of 1210 mol^3 L^{-3} at 20 °C for anhydrous $CaCl_2$, which leads to a solubility of 745 g L^{-1} in water.[42] All of the generated $CaCl_2$ should therefore be in solution, and solubility is of no importance. Since the Ca^{2+} concentration is only 4 g L^{-1}, there must be a restriction in the chemical reaction. The comparison between inorganic acid with HCl and organic acid with citric acid at St 1.0 after 24 h shows that the acid strength of HCl is higher. Accordingly, the ion concentration of citric acid at 981 mg L^{-1} is 4 times lower for the same input quantity. A theoretical change in the microstructure according to Adhiwiguna et al. does not change the leaching behavior.[40]

Influence of the Minerals. After an acid variation, hydrochloric acid shows the largest leaching quantity when used on calcium containing feeds, which is why all further tests are carried out with hydrochloric acid. In addition to anhydrite as a calcium source, talc is present in the mixture as a magnesium source. Figure 3 shows the progression of the Ca^{2+} and Mg^{2+} ion concentrations over the leaching time. The stoichiometric ratios St of hydrochloric acid to the particles are again 0.2, 0.5, and 1.0. The comparison of the calcium leaching of the two minerals anhydrite and talc shows no acid dependence for talc. The calcium value is identical for each acid addition. One explanation for this is that the particle only contains calcium in the impurities, and these are all dissolved with the smallest amount of acid. An increased amount of acid therefore does not change the ion concentration.

Impurities in the particle are also present in anhydrite due to magnesium content, which can be explained according to Table S1, where anhydrite has a MgO content of 0.3%. In general, the leaching kinetics of magnesium from anhydrite is slower, which is shown by the steady increase in the ion concentration. Leaching is therefore not completed after 24 h. Likewise, no significant difference can be observed between the stoichiometric ratios. Thus, there is no advantage for anhydrite with an increased level of acid addition. A similar process can be seen with talc as the magnesium source. A stationary state is also not reached after 24 h of leaching. However, a greater discrepancy can be seen between the stoichiometric ratios. After 24 h of leaching, the magnesium content for St = 1.0 is 277.6 mg L^{-1} and 24% higher than for St = 0.2. For $MgCl_2$, the solubility is 543 g L^{-1} as with $CaCl_2$ much higher than the measured values. This means that only the chemical equilibrium is the limiting factor.[42] However, this is not appropriate in relation to the 5-fold acid quantity. It is therefore also true for talc that the higher acid content does not increase the magnesium yield to the same extent as the amount used. A lower acid input therefore results in a higher efficiency. A comparison of the leaching times with calcium in Figure 2 shows a more sluggish behavior. Even after 24 h, there is still no stationary leaching state. It is irrelevant whether the magnesium ions are dissolved in mineral anhydrite or talc. The curves are identical for both minerals.

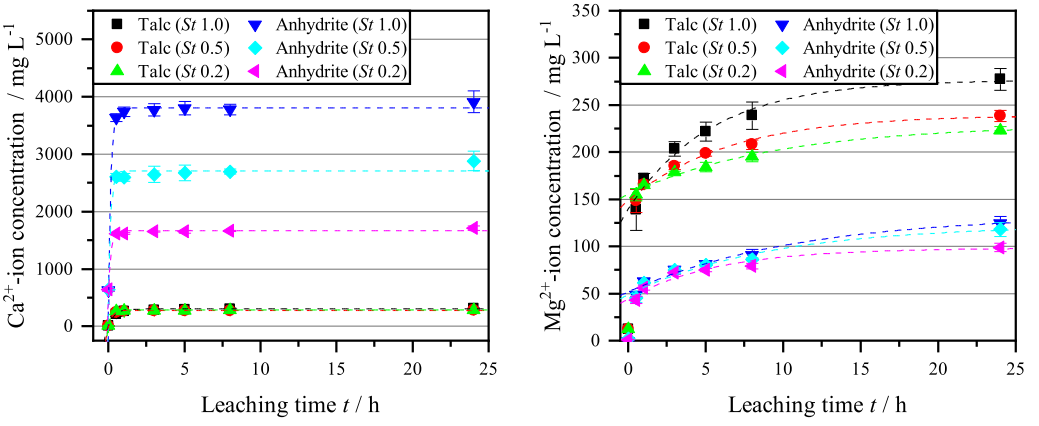

Figure 3. Concentration of Ca^{2+} (left) and Mg^{2+} ions (right) as a function of the leaching time of talc and anhydrite at 5% w/w solids content with hydrochloric acid for the stoichiometric ratios St 0.2, 0.5, and 1.0.

https://doi.org/10.1021/acs.iecr.5c00797
Ind. Eng. Chem. Res. 2025, 64, 12064−12073

The relationship between the minerals can be analyzed in more detail by means of regressions using eq 6. The regression parameters are shown in Table S4 (Supporting Information). When the different parameters of calcium leaching from anhydrite are compared, it can be seen that the values differ only in the stationary concentration $C_{\infty,Ca,An}$. The rate $k_{Ca,An}$ is identical for all stoichiometric ratios, which underlines the independence of $k_{Ca,An}$ from the amount of acid added. For talc, the regression shows no significant differences for any stoichiometric ratio. This proves that calcium leaching is independent of the amount of acid used. Overall, the calcium leaching process can be modeled by eq 6 independent of the particles used, and the solubility in distilled water, the final concentration, and the rate can be derived directly from the regression.

For magnesium, it can be seen that the initial range cannot be represented by a regression. This is shown by the parameter $C_{0,Mg,i}$, which has a value greater than the measured amount of magnesium in distilled water in all of the series of measurements. For all values greater than 0 h, the measuring points can be approximated using eq 6. Therefore, a mathematical definition of the whole leaching process is necessary. The initial range up to 1 h can be described linearly, while the time steps >1 h can be modeled with the same approach as for calcium. When comparing $C_{\infty,Mg,An}$ during leaching of magnesium from anhydrite, the value increases for higher stoichiometric ratios. The rate $k_{Mg,An}$ decreases with an increasing acid concentration. In contrast, the other two parameters, $C_{\infty,Mg,An}$ and $C_{0,Mg,An}$, increase in the same ratio, which explains the similar Mg^{2+} concentrations up to 8 h. Overall, therefore, the leaching of Mg^{2+} is not directly dependent on the amount of acid. Talc leaching shows an increase in the rate $k_{Mg,Ta}$ and concentration at steady state $C_{\infty,Mg,Ta}$. This shows a dependence on acid concentration and pH. First, a higher proportion of magnesium is leached from the particles, and second, the reaction proceeds faster. Both $C_{\infty,Mg,Ta}$ and $k_{Mg,Ta}$ increase linearly with the stoichiometry.

In addition to modeling the leaching, determination of the ion concentration is necessary for control. Due to the kinetics of anhydrite, Ca^{2+} ion determination via chromatography with a measuring time of 30 min is not feasible for control purposes. Here, using an ion selective electrode (ISE) coupled with ion chromatography offers a possible solution to decrease measurement time and allows in-line prediction of Ca^{2+} ion concentration. Coupling the ISE with chromatography or titration is essential, as calcium and magnesium influence each other during the carbonate precipitation, as discussed in the section (anhydrite carbonate precipitation).

Measuring conductivity by adding acid is not expedient. Figure 4 shows the temporal change in conductivity for the investigated particle systems at a time interval of 1 min. Acid is added after 60 min. A sudden increase in conductivity can be seen when the acid is added, which then remains constant. In the case of talc, in particular, leaching is not yet complete according to Figure 3, which cannot be read from the conductivity. The change in ion concentration can therefore not be estimated from the conductivity. However, the fluctuating values in the conductivity, which are due to foaming of the suspension, are striking. Without the addition of acid, the ion concentration can be estimated via the conductivity, as this increases via free ions in the solution. Table S5 (Supporting Information) shows the measured ion concentrations of Ca^{2+} and Mg^{2+} in the ion chromatography

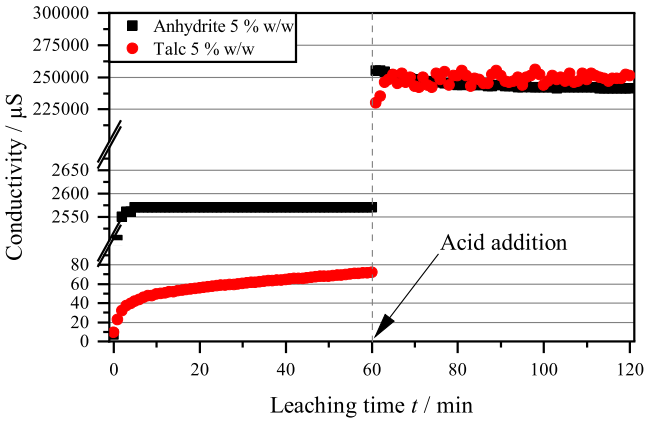

Figure 4. Conductivity measurement for determining the solubility of particles of talc and anhydrite without the addition of acid (0−60 min) and after the addition of acid (61−120 min).

after 1 min in deionized water and after 60 min in deionized water. After the addition of acid, a measured value was recorded again after a further 60 min. For anhydrite, the Ca^{2+} concentration is 14-times higher than for Talc. Regarding the Mg^{2+} concentration, Talc has a 2.7 times higher concentration than Anhydrite. These changes cannot be seen with measuring the conductivity of the suspension.

When looking at the leaching of Ca and Mg from both minerals, Figure 3 shows a difference between the two alkaline earth metals. While calcium is in the stationary end range after 30 min, the leaching of magnesium is not yet complete after 24 h. As both minerals are relevant, the further leaching time was set at 3 h. Therefore, the following experiments are carried out to investigate the influence of mass at a leaching time of 3 h. Figure 5 shows the influence of the particle mass concentration on the leaching quality. Noticeable are the values of $C_{Ca,Ta}$* and $C_{Mg,An}$*, which are both above the value of 1. This is not plausible because it means a higher ion content in the solution than the ion content of the added particles. The only explanation is the loss of ignition (LOI), which is 1% of the particle mass for anhydrite and 5% for talc; see Table S1. These components must include both calcium and magnesium. The high LOI content of talc is reflected in the Ca^{2+} values, which are up to 1.5 times the theoretical amount of calcium. In the case of anhydrite, the Mg^{2+} values are only above 100% at St = 1, but this corresponds to only 3 h of leaching. After 24 h of leaching, all the measured values are $C_{Mg,An}$* > 1, which is only possible due to trace elements in the organic residues. The exact proportion of calcium and magnesium from the trace elements cannot be determined with the method described here.

With regard to the influence of different mass concentrations on magnesium leaching, the behavior is similar to that of calcium with talc. Regardless of the acid concentration in the solution, the identical ion concentration ratio $C_{Mg,Ta}$* is present after 3 h of leaching in Figure 5 (right) and all $C_{Mg,An}$* values are within a same range, too. However, Figure 3 shows that leaching is not yet complete after 3 h. This means that the reaction rate is not dependent on the acid concentration. However, the same concentration ratio C_i* means a linear increase of Mg^{2+} with the mass concentration in the suspension. Three times the amount of particles also corresponds to three times the amount of dissolved magnesium after 3 h. This behavior is reflected in both

https://doi.org/10.1021/acs.iecr.5c00797
Ind. Eng. Chem. Res. 2025, 64, 12064−12073

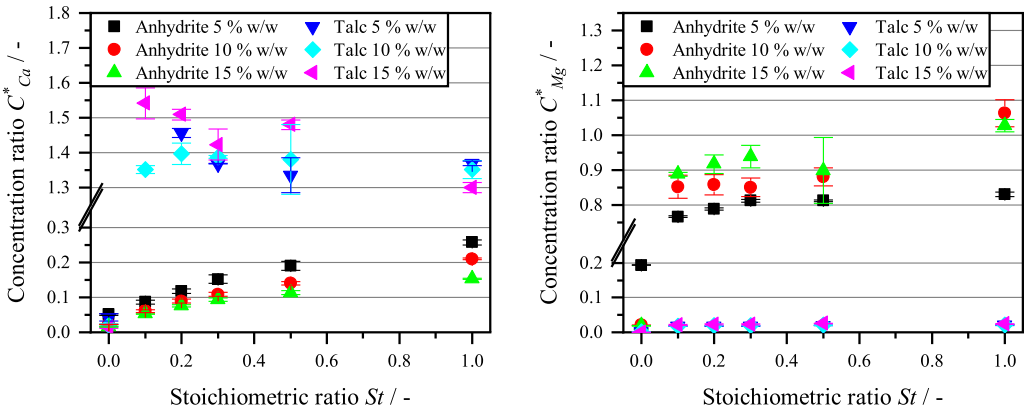

Figure 5. Influence of the mass concentration and acid quantity of hydrochloric acid on the normalized amount of Ca^{2+} (left) and Mg^{2+} ions (right) leached.

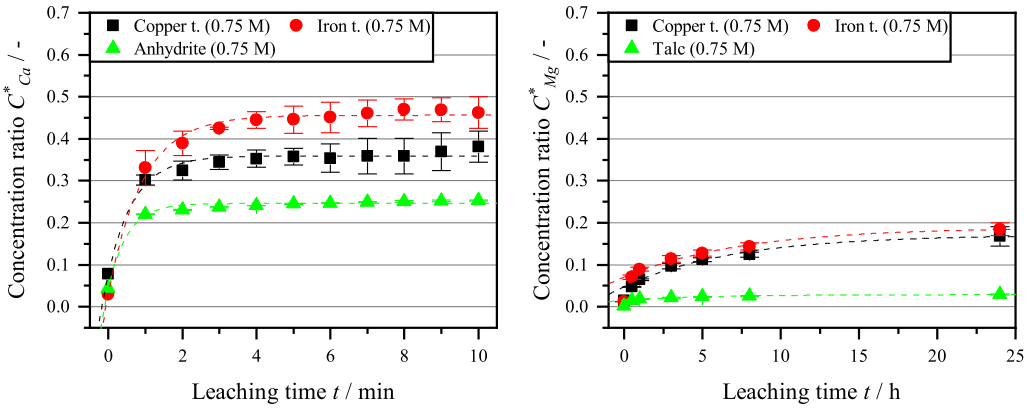

Figure 6. Leaching of the tailings as a function of leaching time t. On the left, the comparison of Ca with anhydrite as the calcium source, and on the right, the comparison of Mg with talc as the magnesium source.

anhydrite and talc. Therefore, there is a proportional behavior between the mass concentration of particles and the amount of magnesium leached, whereas the acid concentration shows no dependence on the leaching rate. Whether the leached magnesium ion concentration in the steady state is dependent on the amount of acid needs to be investigated in a further study.

Regarding $C_{Ca,An}$*, an increasing stoichiometric ratio increases the amount of Ca^{2+} ions within the solution. Anhydrite is, in theory, completely soluble in acid. However, as it does not dissolve completely, the leaching reaches the chemical equilibrium, since the solubility of $CaCl_2$ is with 745 g L^{-1} higher than the measured values.[42] This is dependent on the temperature and pH value. However, the temperature is kept constant in all experiments at T = 25 °C. The measured pH values are listed in Table S6 (Supporting Information). A higher stoichiometric ratio implies a shift in the chemical equilibrium and a lower pH. Therefore, it should be possible to express the change in the Ca^{2+} concentration by measuring the pH, as shown in Table S6. This explains the increase in $C_{Ca,An}$* for higher St. Contrary to expectations, the percentage of dissolved calcium from particles with higher mass concentrations decreases. However, the total amount of dissolved calcium at higher mass concentrations has increased. For example, at St = 1.0, between 5 and 15% w/w, $C_{Ca,An}$* is greater by a factor of 1.68, while at 15% w/w, $c_{Ca,max}$ increases by a factor of 3. Thus, the absolute amount of calcium increases, while the percentage of calcium decreases. Double the amount of acid and particles does not mean double the amount of dissolved ions. For this reason, it is advantageous to use smaller amounts of particles and acid for the process.

A comparison of the individual pH values in Table S6 shows a decrease with a higher acid content and mass concentration. As the mass concentration increases and the stoichiometric ratio remains constant, the amount of acid added also increases, causing the pH value of the solution to decrease. Compared with anhydrite, the pH values for talc are generally in the same range. Due to its more complex mineral structure, talc has a molar mass of 379.26 g mol^{-1}, 2.76 times higher than the molar mass of anhydrite at 136.14 g mol^{-1}. This results in only one-third of the molar mass for the same mass concentration. However, according to reaction eq 2, the amount of acid also increases by a factor of 3. The amount of acid used for both minerals is therefore in a similar range and explains the little difference between both alkaline ions. The only noticeable difference is at stoichiometry 0, where no acid is added, which is why only the solubility of the minerals in water has an effect on the pH value. In the case of anhydrite, this is in the neutral range of pH 7, while talc has a slightly basic pH value of 8. According to Lin and Cemency, talc has a basic character, which explains this pH value.[43]

Investigation of Tailings. In addition to the individual particles, two tailings are examined and compared as a function of leaching time and acid amount. Since an explicit reaction equation cannot be written for tailings, the same acid amounts are used as for anhydrite. At 5 mass percent, the equivalent for

https://doi.org/10.1021/acs.iecr.5c00797
Ind. Eng. Chem. Res. 2025, 64, 12064−12073

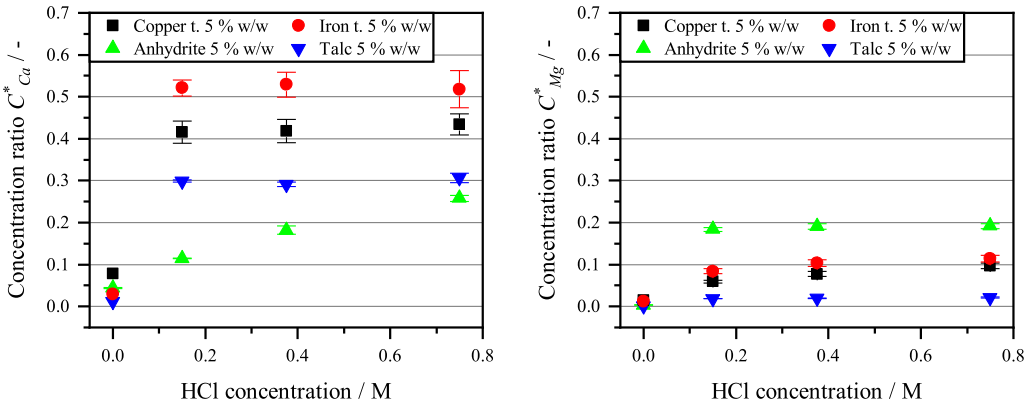

Figure 7. Comparison of the leaching (leaching time 3 h) of tailings with the individual particles as a function of the molar amount of HCl. Left for calcium and right for magnesium.

St = 1 is 0.75 M HCl. Figure 6 shows the fraction of dissolved ions from the particles. According to Figure 1, a steady state for calcium determination is reached after 30 min, so the measuring intervals are reduced to one measuring point per minute. After 1 min, the anhydrite has already reached 85% of the steady-state value, while the copper tailing has only reached 75%, even though both use the same mineral as a source of calcium. Furthermore, only 25% of the calcium contained in the mineral can be dissolved in anhydrite, while 38% can be dissolved in copper tailings. This can be explained by the chemical equilibrium, as is the case with anhydrite; see Figure 2. However, this value is not reached in copper tailings. Here, after 10 min, only 360 mg L^{-1} dissolve, which is one-tenth of the 3700 mg L^{-1} reached in anhydrite. Therefore, other minerals are interfering with the process. There is no significant difference in the speed of the leaching process, which can be attributed to the identical minerals.

In the iron tailings, calcite is the main source of calcium and, therefore, the target product. However, it is bound to other mineral structures and cannot be used in this form, so leaching is a necessary step. As with copper tailings and anhydrite, a large proportion of the steady-state value, 70%, is released within the first minute. Overall, the leaching of calcite from iron tailings is slower than the leaching of gypsum from copper tailings. However, with 640 mg L^{-1}, 1.78 times more calcium is leached in absolute terms, and with $C_{Ca,Fe}{}^* = 0.47$, 10% more is leached compared to copper tailings.

Figure 4 shows that talc is a stable mineral against acid, which is why leaching is not complete even after 24 h, in contrast to calcium extraction. Figure 6 (right) also shows the low yield of magnesium at 3% of the amount used. With such a small amount, it is likely that it is not the dissolved talc but the trace elements of the organic components. In the two tailings, no explicit minerals can be assigned to the magnesium content, making the prediction difficult. However, it is noticeable that the leaching is not complete after 24 h and that the decreasing trend is similar to those of talc and anhydrite. A similar proportion of the magnesium present is leached from both tailings with $C_{Mg,i}{}^* = 0.17$. The iron tailings contain 1.5 times the amount of Mg^{2+} according to Table S2, which means that the proportion has no effect on the chemical equilibrium. However, the 17% leaching of magnesium with HCl is small compared to the more than 70% leaching with H_2SO_4 and serpentine.[28] HCl has a higher yield for calcium leaching, and H_2SO_4 has a higher yield for magnesium leaching. In order to obtain both with a high yield, a two-step process may be useful in the future.

Using regression according to eq 6, the initial range cannot be represented in a way comparable to that of the individual particles. However, the initial range can be described by a linear function up to 1 h. By comparing the rates $k_{Mg,i}$, a common characteristic can be determined, see Table S7 (Supporting Information). The values for all measured particles and particle-acid mixtures are between 0.1 and 0.2, which describes a similar reaction character independent of the particle system. A similar behavior is observed when the rates $k_{Ca,i}$. The reaction is very fast for all measured particle systems, which is reflected in the values in the same size range of $k_{Ca,i}$ = 5 h^{-1}. Therefore, no predictions about the reaction rate can be made by measuring individual particle systems. The situation is different for the amount of ions in solution. The coefficient $C_{\infty,Ca,i}$ shows the amount of calcium dissolved in the two tailings, which does not change regardless of the acid concentration used. This is in contrast to anhydrite, although the copper tailings contain identical mineral gypsum. The fact that calcium is independent of the acid concentration indicates that there is calcium in the particles that cannot be extracted. The same is the case for the iron tailings. The extractable ion concentration does not change with the amount of acid.

This is shown graphically in Figure 7 (left). The amount of calcium with an increasing acid amount changes only for anhydrite. For the two tailings and talc, smaller amounts of acid are more effective. With regard to magnesium leaching (Figure 7, right), a different behavior between the individual particles and the tailings is shown. For the individual particles, there is no increase in the rate with increasing amounts of acid. For the tailings, however, the leaching rate increases. This is not apparent from the regression parameters shown in Table S7 due to the small number of data points. The regression for magnesium is therefore less precise, especially in the initial range.

Anhydrite Carbonate Precipitation. The carbon capture process using the mine tailings as carbonate compounds, as mentioned earlier, is a 4-step process where the leaching and filtration are followed by precipitation and, finally, separation of the products. This section uses one example to show that the process chain to produce valuable carbonates from mining waste is possible. The mine tailings contain various ions along with the necessary Ca^{2+} and Mg^{2+} ions needed for the precipitation of the value products, $CaCO_3$ and $MgCO_3$. This requires that the pure carbonates are precipitated selectively

https://doi.org/10.1021/acs.iecr.5c00797
Ind. Eng. Chem. Res. 2025, 64, 12064−12073

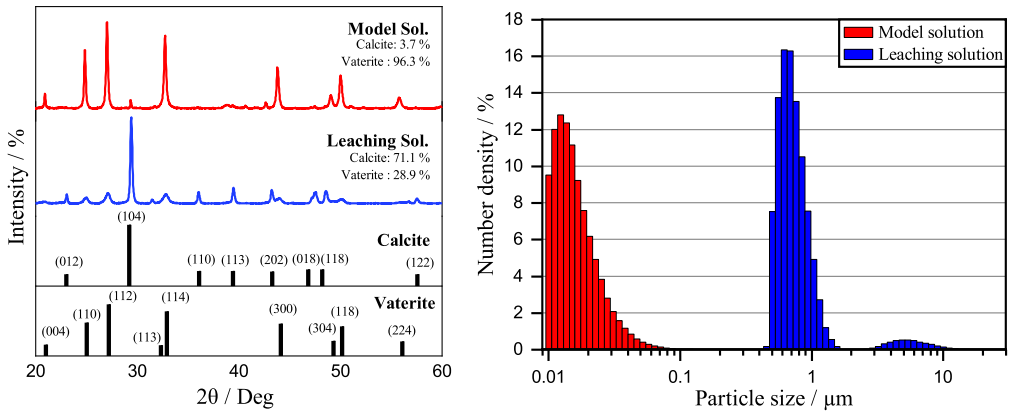

Figure 8. XRD analysis (left) and PSD analysis (right) for $CaCO_3$ precipitation using the extracted solution (Anhydrite, St. 1.0) (blue) and an equimolar model solution (red).

one after the other and separated from the solution. The method used for the carbonate precipitation is pH-swing[44] since the leaching of the ions takes place at low pH conditions, while the precipitation of the carbonates happens at high pH conditions where the solubility of $CaCO_3$ and $MgCO_3$ is quite low[44] and almost all the carbonates formed can be precipitated and separated from the solution. After the leaching of the Ca^{2+} and Mg^{2+} ions from the solutions of anhydrite, clear solutions are filtered and used for the next step of precipitation in the carbon dioxide sequestration process at the partner university, Otto-von-Guericke University, Magdeburg. For the pH shift from low to high, 1 M NaOH solution, prepared using solid NaOH from Merck KGaA (Darmstadt, Germany), was added continuously at 2.5 mL min^{-1} to 300 mL anhydrite extract at St = 1.0. While the NaOH solution was added, pH and Ca^{2+} ion concentration were measured using the pH Sensor InLab Expert and DX240-Ca ISE, both Mettler Toledo make. The ISE sensor is only used to understand dynamic changes in concentration during the experiment. IC measurements are more accurate, but the analysis takes longer and there is a delay for control. The CO_2 needed for the carbonation was supplied to the solution by bubbling the CO_2 gas (99.5% pure), from Linde GmbH (Pullach, Germany), at a constant rate during the pH shift process into the closed tank for precipitation. To extract pure carbonates selectively through the pH swing process, first, $CaCO_3$ was precipitated since the solubility of $CaCO_3$ is much lower than that of $MgCO_3$. The pH of the anhydrite extracted solution, which is initially at a very low pH, is increased until pH 8 and maintained at this pH by the continuous supply of CO_2 and NaOH until the Ca^{2+} concentration (measured using Ca ISE) in the solution is almost zero. After extracting the precipitated $CaCO_3$, the pH of the solution was further increased to around pH 9.5 where the hydrated forms of $MgCO_3$ would precipitate. However, since the concentration of Mg^{2+} was too low in the anhydrite solution, no carbonates of magnesium could be precipitated. The saturation of $MgCO_3$ at pH 9.5 is 1.8×10^{-4} mol L^{-1}, which means that the concentration of Mg^{2+} is 4.4 mg L^{-1}. Therefore, a small amount should have been precipitated, but since only a small amount of liquid was used, no $MgCO_3$ could be measured. Of course, the saturation is highly dependent on the pH value and changes accordingly. For $CaCO_3$, the saturation at pH 9.5 is 1.6×10^{-6} mol L^{-1} and for Ca^{2+} 64 μg L^{-1}. This should make over 99% of the leached alkaline metal ions available for precipitation.

The PCC was collected and analyzed qualitatively and quantitatively. The morphology of the $CaCO_3$ was analyzed using the D2 Phaser X-ray Diffraction (XRD) from Bruker Corporation (Massachusetts, United States), the results of which are shown in Figure 8 (left). The particle size of the precipitates was measured using a Mastersizer 3000 Hydro HV from Malvern Panalytical. The mean size of the particles was around 0.74 μm (Figure 8, right). The experiment was repeated using a model solution, equimolar in concentrations of Ca^{2+} and Mg^{2+} as that of the Anhydrite solution, prepared using pure $CaCl_2{\cdot}2H_20$ and $MgCl_2$ from Carl Roth GmbH + Co. KG (Karlsruhe, Germany). The XRD analysis of the two samples in Figure 8 (left) shows that for the extracted anhydrite solution, primarily, the cubic structured, large calcite crystals are precipitated with a small amount of hexagonal-shaped Vaterite. While the precipitation using the model solution in Figure 8 (right) showed that smaller, metastable Vaterite crystals are precipitated almost completely, which, over time, changes to the more stable calcite particles, as also been mentioned by Ngu et al., 2019.[45] This shows that the morphology of the precipitated $CaCO_3$ is dictated by the presence of other impurities in the solution, as also mentioned in[46]. The study to analyze and model this in more detail is in progress and will be presented in the future. In both cases, however, no $MgCO_3$ could be precipitated due to the low concentration of Mg^{2+} and higher solubility in the solutions.

CONCLUSION

In this paper, the leaching from two individual particles and two tailings are characterized. The target products are calcium and magnesium ions at the highest possible concentration. The experiments have shown that hydrochloric acid results in a higher leached amount of calcium and magnesium due to the higher solubility of chlorides. Sulfuric acid, on the other hand, has a reaction partner through the combination with anhydrite, in which sulfate is formed as an anion by both reactants, which is why this cannot react. Compared to hydrochloric acid, citric acid as an organic acid produces only a third of the ion concentration of calcium with the same amount used. The use of sulfuric acid and citric acid shows that the increase in ion concentration is dependent on not only the pH value but also microstructural changes within anhydrite.

Higher mass concentrations with the same stoichiometric ratio also mean a higher leached quantity of alkaline ions. In the case of anhydrite, this is limited by the chemical

https://doi.org/10.1021/acs.iecr.5c00797
Ind. Eng. Chem. Res. 2025, 64, 12064−12073

equilibrium, which is validated by measuring the pH value. A lower pH value therefore means a higher calcium content in the solution and, correspondingly, a higher final quantity of dissolved ions.

Compared with anhydrite, talc reacts more slowly. While anhydrite has reached its stationary range after 2 min, an increase in the ion concentration can still be seen in talc after 24 h. The reaction rate for talc increases with a higher acid concentration. The leaching of both calcium and magnesium ions can be described using eq 6. The value $k_{Mg,i}$ shows here a disproportionate increase in rate with the amount of acid. For anhydrite, the rate is independent of the amount of acid.

The higher calcium leaching at a lower pH cannot be demonstrated for mine waste. Only 38% of the calcium content from the copper mine and 47% from the iron mine can be leached from both tailings. This maximum is also independent of acidity; therefore, it must be due to unavailable calcium. To make more calcium available, grinding tailings may help. More magnesium can be dissolved from the tailings than from the talc. This can be explained by the chemical resistance of talc to the acid. Both target products, Ca^{2+} and Mg^{2+}, behave the same in terms of leaching rate with the rates of the individual particles.

For storing and utilizing atmospheric CO_2 in the form of carbonates, the pH swing precipitation process showed that the anhydrite solution is suitable for the production of $CaCO_3$, which makes anhydrite containing waste steams a possible source for carbonation. For the precipitation of $MgCO_3$, the concentration of magnesium needs to be increased in both the anhydrite and talc solutions. This is also a limitation of this method. Depending on the acid−mineral combination used, there is only a limited amount of ions in the solution. With our tailings and HCl, the tailings were only 17% for Mg^{2+}. The literature mentions 70% for H_2SO_4 in serpentine. In addition, the yield of ions increases with a larger pH shift from acidic to basic because the saturation for both leaching and precipitation is pH dependent. At the same time, more reagents are required for a larger pH shift, making this an economic optimization problem for each individual reagent and product combination. In general, the experiments show that the extraction of calcium and magnesium from mineral particles can be described using a simple exponential expression approach and can therefore be used for autonomous control of the carbonation process. As a process improvement, after precipitation and separation of all generated carbonates, NaOH and HCl can be recovered by direct electrosynthesis.[47] Through electrosynthesis, the product chain for HCl (leaching) and NaOH (precipitation) would be closed. Energy efficiency and scalability will be addressed after merging the complete process chain and integration of a model-based autonomous controller to run the process under optimal conditions.

■ ASSOCIATED CONTENT

Data Availability Statement

The data that supported the results of this study can be found on KITopen/Radar4KIT under the following DOI as open source and freely accessible: 10.35097/1g4v0wv0crcc0brv

Supporting Information

The Supporting Information is available free of charge at https://pubs.acs.org/doi/10.1021/acs.iecr.5c00797.

Chemical composition of the product; mass-based composition of the used tailings; calculated maximum concentrations $c_{i,theo\ max}$ of calcium and magnesium; determined coefficients $C_{\infty,i,}$ $C_{0,i,\ and}$ k_i; solubility of Ca_{2+} and Mg_{2+} for the pure minerals; measured pH values of the solutions; and determined coefficients C∞,i, C0,i, and ki (PDF)

■ AUTHOR INFORMATION

Corresponding Authors

Volker Bächle − *Institute of Mechanical Process Engineering and Mechanics, Karlsruhe Institute of Technology (KIT), 76131 Karlsruhe, Germany*; orcid.org/0000-0001-8708-3408; Email: volker.baechle@kit.edu

Marco Gleiß − *Institute of Mechanical Process Engineering and Mechanics, Karlsruhe Institute of Technology (KIT), 76131 Karlsruhe, Germany*; Email: marco.gleiss@kit.edu

Authors

Chinmay Laxminarayan Hegde − *Institute of Process Systems Engineering, Otto-von-Guericke University Magdeburg (OVGU), 39106 Magdeburg, Germany*

Andreas Voigt − *Institute of Process Systems Engineering, Otto-von-Guericke University Magdeburg (OVGU), 39106 Magdeburg, Germany*

Kai Sundmacher − *Institute of Process Systems Engineering, Otto-von-Guericke University Magdeburg (OVGU), 39106 Magdeburg, Germany*; orcid.org/0009-0008-8156-0611

Complete contact information is available at: https://pubs.acs.org/10.1021/acs.iecr.5c00797

Notes

This work is published nonpeer-review as a preprint on the ChemRxiv server according to the ACS Publication regulations with the corresponding DOI: 10.26434/chemrxiv-2025-cjxfm. The authors declare no competing financial interest.

■ ACKNOWLEDGMENTS

The authors would like to thank the Deutsche Forschungsgemeinschaft (DFG, German Research Foundation)—Project number: 504852622 for funding the project in the priority program autonomous processes in particle technology SPP 2364.

■ REFERENCES

(1) Krevor, S. C.; Lackner, K. S. Enhancing Process Kinetics for Mineral Carbon Sequestration. *Energy Procedia* **2009**, *1* (1), 4867−4871.

(2) *Calciumcarbonat: von der Kreidezeit ins 21. Jahrhundert*; Tegethoff, F. W., Rohleder, J., Eds.; Birkhäuser: Basel Boston Berlin, 2001.

(3) Han, Y. S.; Hadiko, G.; Fuji, M.; Takahashi, M. Effect of Flow Rate and CO2 Content on the Phase and Morphology of CaCO3 Prepared by Bubbling Method. *J. Cryst. Growth* **2005**, *276* (3−4), 541−548.

(4) Jimoh, O. A.; Ariffin, K. S.; Hussin, H. B.; Temitope, A. E. Synthesis of Precipitated Calcium Carbonate: A Review. *Carbonates Evaporites* **2018**, *33* (2), 331−346.

(5) *Environmental Processes and Management: Tools and Practices*; Singh, R. M., Shukla, P., Singh, P., Eds.; *Water science and technology library*; Springer: Cham, Switzerland, 2020; Vol. *1*.

(6) Moropoulou, A.; Bakolas, A.; Aggelakopoulou, E. The Effects of Limestone Characteristics and Calcination Temperature to the Reactivity of the Quicklime. *Cem. Concr. Res.* **2001**, *31* (4), 633−639.

(7) Wang, L. K. Advanced Physicochemical Treatment Technologies. In *Handbook of Environmental Engineering*; Hung, Y.-T., Shammas, N. K., Eds.; Humana Press: Totowa, NJ, 2007; ..
(8) Woodall, C. M. *A Multi-Faceted Approach to Carbon Mineralization Advancement*. PhD Thesis, Worcester Polytechnic Institute, 2021.
(9) Chen, Z.; Song, H. S.; Portillo, M.; Lim, C. J.; Grace, J. R.; Anthony, E. J. Long-Term Calcination/Carbonation Cycling and Thermal Pretreatment for CO_2 Capture by Limestone and Dolomite. *Energy Fuels* **2009**, *23* (3), 1437−1444.
(10) Snæbjörnsdóttir, S. O.ˊ.; Sigfússon, B.; Marieni, C.; Goldberg, D.; Gislason, S. R.; Oelkers, E. H. Carbon Dioxide Storage through Mineral Carbonation. *Nat. Rev. Earth Environ.* **2020**, *1* (2), 90−102.
(11) Azdarpour, A.; Asadullah, M.; Mohammadian, E.; Hamidi, H.; Junin, R.; Karaei, M. A. A Review on Carbon Dioxide Mineral Carbonation through pH-Swing Process. *Chem. Eng. J.* **2015**, *279*, 615−630.
(12) Bobicki, E. R.; Liu, Q.; Xu, Z.; Zeng, H. Carbon Capture and Storage Using Alkaline Industrial Wastes. *Prog. Energy Combust. Sci.* **2012**, *38* (2), 302−320.
(13) Wilcox, J. *Carbon Capture*; Springer New York: New York, NY, 2012; ..
(14) Yao, Z. T.; Ji, X. S.; Sarker, P. K.; Tang, J. H.; Ge, L. Q.; Xia, M. S.; Xi, Y. Q. A Comprehensive Review on the Applications of Coal Fly Ash. *Earth-Sci. Rev.* **2015**, *141*, 105−121.
(15) Singh, A.; Kelkar, N.; Natarajan, K.; Selvaraj, S. Review on the Extraction of Calcium Supplements from Eggshells to Combat Waste Generation and Chronic Calcium Deficiency. *Environ. Sci. Pollut. Res.* **2021**, *28* (34), 46985−46998.
(16) Katsuyama, Y.; Yamasaki, A.; Iizuka, A.; Fujii, M.; Kumagai, K.; Yanagisawa, Y. Development of a Process for Producing High-purity Calcium Carbonate ($CaCO_3$) from Waste Cement Using Pressurized CO_2. *Environ. Prog.* **2005**, *24* (2), 162−170.
(17) Sahoo, P. K.; Kim, K.; Powell, M. A.; Equeenuddin, S. M. Recovery of Metals and Other Beneficial Products from Coal Fly Ash: A Sustainable Approach for Fly Ash Management. *Int. J. Coal Sci. Technol.* **2016**, *3* (3), 267−283.
(18) Lee, S. M.; Lee, S. H.; Jeong, S. K.; Youn, M. H.; Nguyen, D. D.; Chang, S. W.; Kim, S. S. Calcium Extraction from Steelmaking Slag and Production of Precipitated Calcium Carbonate from Calcium Oxide for Carbon Dioxide Fixation. *J. Ind. Eng. Chem.* **2017**, *53*, 233−240.
(19) Golik, V. I.; Klyuev, R. V.; Martyushev, N. V.; Brigida, V.; Efremenkov, E. A.; Sorokova, S. N.; Mengxu, Q. Tailings Utilization and Zinc Extraction Based on Mechanochemical Activation. *Materials* **2023**, *16* (2), 726.
(20) Santibáñez-Velásquez, L. E.; Guzmán, A.; Morel, M. J. Extraction of Iron and Other Metals from Copper Tailings through Leaching. *Metals* **2022**, *12* (11), 1924.
(21) Goff, F.; Lackner, K. S. Carbon Dioxide Sequestering Using Ultramaf Ic Rocks. *Environ. Geosci.* **1998**, *5* (3), 89−102.
(22) Gerdemann, S. J.; O'Connor, W. K.; Dahlin, D. C.; Penner, L. R.; Rush, H. Ex Situ Aqueous Mineral Carbonation. *Environ. Sci. Technol.* **2007**, *41* (7), 2587−2593.
(23) Hitch, M.; Ballantyne, S. M.; Hindle, S. R. Revaluing Mine Waste Rock for Carbon Capture and Storage. *Int. J. Min., Reclam. Environ.* **2010**, *24* (1), 64−79.
(24) Jacobs, A. D.; Hitch, M. Experimental Mineral Carbonation: Approaches to Accelerate CO_2 Sequestration in Mine Waste Materials. *Int. J. Min., Reclam. Environ.* **2011**, *25* (4), 321−331.
(25) Jacobs, A.; Hitch, M.; Mosallanejad, S.; Bhatelia, T.; Li, J.; Farhang, F. Mineral Carbonation Potential (MCP) of Mine Waste Material: Derivation of an MCP Parameter. *Minerals* **2023**, *13* (9), 1129.
(26) Li, J.; Hitch, M. Carbon Dioxide Adsorption Isotherm Study on Mine Waste for Integrated CO 2 Capture and Sequestration Processes. *Powder Technol.* **2016**, *291*, 408−413.
(27) Li, J.; Hitch, M. Structural and Chemical Changes in Mine Waste Mechanically-Activated in Various Milling Environments. *Powder Technol.* **2017**, *308*, 13−19.
(28) Li, J.; Hitch, M.; Power, I.; Pan, Y. Integrated Mineral Carbonation of Ultramafic Mine Deposits—A Review. *Minerals* **2018**, *8* (4), 147.
(29) Veetil, S. P.; Hitch, M. Recent Developments and Challenges of Aqueous Mineral Carbonation: A Review. *Int. J. Environ. Sci. Technol.* **2020**, *17* (10), 4359−4380.
(30) Bullock, L. A.; James, R. H.; Matter, J.; Renforth, P.; Teagle, D. A. H. Global Carbon Dioxide Removal Potential of Waste Materials From Metal and Diamond Mining. *Front. Clim.* **2021**, *3*, 694175.
(31) Renforth, P. The Negative Emission Potential of Alkaline Materials. *Nat. Commun.* **2019**, *10* (1), 1401.
(32) Zhang, J.; Zhang, R.; Geerlings, H.; Bi, J. A Novel Indirect Wollastonite Carbonation Route for CO_2 Sequestration. *Chem. Eng. Technol.* **2010**, *33* (7), 1177−1183.
(33) Sabine, C. L.; Heimann, M.; Artaxo, P.; Bakker, D. C.; Chen, C.-T. A.; Field, C. B.; Gruber, N.; Le Quéré, C.; Prinn, R. G.; Richey, J. E.; , et al. Current Status and Past Trends of the Global Carbon Cycle. In *Glob. Carbon Cycle Integrating Hum. Clim. Nat. World*; Island Press, 2004; Vol. *62*, pp 17−44.
(34) Anlauf, H. *Wet Cake Filtration: Fundamentals, Equipment, and Strategies*; Wiley VCH: Weinheim, Germany, 2019; ..
(35) Olajire, A. A. A Review of Mineral Carbonation Technology in Sequestration of CO2. *J. Pet. Sci. Eng.* **2013**, *109*, 364−392.
(36) Saldi, G. D.; Köhler, S. J.; Marty, N.; Oelkers, E. H. Dissolution Rates of Talc as a Function of Solution Composition, pH and Temperature. *Geochim. Cosmochim. Acta* **2007**, *71* (14), 3446−3457.
(37) Li, Z.; Demopoulos, G. P. Solubility of $CaSO_4$ Phases in Aqueous HCl + $CaCl_2$ Solutions from 283 to 353 K. *J. Chem. Eng. Data* **2005**, *50* (6), 1971−1982.
(38) Li, Z.; Demopoulos, G. P. Development of an Improved Chemical Model for the Estimation of $CaSO_4$ Solubilities in the HCl−$CaCl_2$ − H_2 O System up to 100 °C. *Ind. Eng. Chem. Res.* **2006**, *45* (9), 2914−2922.
(39) Castellón, F. J.; Ayala, M.; Flores, J. A.; Lanzón, M. Influence of Citric Acid on the Fire Behavior of Gypsum Coatings of Construction and Structural Elements. *Mater. Constr.* **2021**, *71* (342), No. e248.
(40) Adhiwiguna, I. B. G. S.; Yu, X.; Warnecke, R.; Deike, R. Citric Acid-Based Treatment for Refining Mineral Fractions Recovered from Processed MSW Incinerator Bottom Ash. *Appl. Sci.* **2025**, *15* (1), 249.
(41) VDI. *VDI 2762 Part 2. Mechanical Solid-Liquid Separation by Cake Filtration. Determination of Filter Cake Resistance*, 2010.
(42) Lide, D. R.; Baysinger, G.; Chemistry, S.; Berger, L. I.; Goldberg, R. N.; Kehiaian, H. V. *CRC Handbook of Chemistry and Physics*, 83 ed.; CRC Press: Boca Raton, FL, 2005.
(43) Lin, F.-C.; Clemency, C. V. The Dissolution Kinetics of Brucite, Antigorite, Talc, and Phlogopite at Room Temperature and Pressure. *Am. Mineral.* **1981**, *66* (7−8), 801−806.
(44) Hegde, C.; Voigt, A.; Sundmacher, K. Towards pH Swing-based CO2 Mineralization by Calcium Carbonate Precipitation: Modeling and Experimental Analysis. In *Computer Aided Chemical Engineering*; Elsevier, 2024; Vol. *53*, pp 1519−1524..
(45) Ngu, L.; Song, J. W.; Hashim, S. S.; Ong, D. E. Lab-scale Atmospheric CO_2 Absorption for Calcium Carbonate Precipitation in Sand. *Greenhouse Gases:Sci. Technol.* **2019**, *9* (3), 519−528.
(46) Liendo, F.; Arduino, M.; Deorsola, F. A.; Bensaid, S. Nucleation and Growth Kinetics of CaCO3 Crystals in the Presence of Foreign Monovalent Ions. *J. Cryst. Growth* **2022**, *578*, 126406.
(47) Kumar, A.; Phillips, K. R.; Thiel, G. P.; Schröder, U.; Lienhard, J. H. Direct Electrosynthesis of Sodium Hydroxide and Hydrochloric Acid from Brine Streams. *Nat. Catal.* **2019**, *2* (2), 106−113.

https://doi.org/10.1021/acs.iecr.5c00797
Ind. Eng. Chem. Res. 2025, 64, 12064−12073